Effect of Biochar on Microbial Growth: A Metabolomics and Bacteriological Investigation in *E. coli*

Rebecca A. Hill, **John Hunt**, **Emily Sanders**, **Melanie Tran**, **Griffin A. Burk**, **Todd E. Mlsna**, and **Nicholas C. Fitzkee**[*]

Department of Chemistry, Mississippi State University, Mississippi State, MS 39762

Abstract

Biochar has been proposed as a soil amendment in agricultural applications due to its advantageous adsorptive properties, high porosity, and low cost. These properties allow biochar to retain soil nutrients, yet the effects of biochar on bacterial growth remain poorly understood. To examine how biochar influences microbial metabolism, *Escherichia coli* was grown in a complex, well-defined media and treated with either biochar or activated carbon. The concentration of metabolites in the media were then quantified at several time points using NMR spectroscopy. Several metabolites were immediately adsorbed by the char, including L-asparagine, L-glutamine, and L-arginine. However, we find that biochar quantitatively adsorbs less of these metabolic precursors when compared to activated carbon. Electron microscopy reveals differences in surface morphology after cell culture, suggesting that *Escherichia coli* can form biofilms on the surfaces of the biochar. An examination of significant compounds in the tricarboxylic acid cycle and glycolysis reveals that treatment with biochar is less disruptive than activated carbon throughout metabolism. While both biochar and activated carbon slowed growth compared to untreated media, *Escherichia coli* in biochar-treated media grew more efficiently, as indicated by a longer logarithmic growth phase and a higher final cell density. This work suggests that biochar can serve as a beneficial soil amendment while minimizing the impact on bacterial viability. In addition, the experiments identify a mechanism for biochar's effectiveness in soil conditioning and reveal how biochar can alter specific bacterial metabolic pathways.

Graphical Abstract

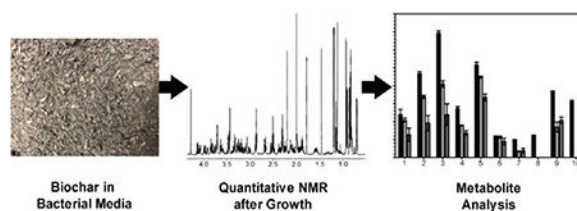[*]**Corresponding Author:** To whom correspondence should be addressed. nfitzkee@chemistry.msstate.edu.

Biochar in Bacterial Media → Quantitative NMR after Growth → Metabolite Analysis

Keywords

^{1}H NMR spectroscopy; Metabolomics; Biochar; *Escherichia coli*

INTRODUCTION

Biochar (BC) is often produced from renewable organic waste that is converted to a carbonaceous material through pyrolysis and it is comparatively cheaper than activated carbon (AC).[1–3] BC, a carbon source, is often used in agriculture as a soil additive due to its adsorptive properties, porous surface, and low cost. BC improves soil fertility and structure, sequesters carbon (mitigating climate change), and enriches beneficial soil microorganisms. [4–9] BC's adsorptive properties vary with feedstock and pyrolysis conditions, which can be tailored for optimal removal of specific chemicals, such as pesticides, phosphates, organic dyes, heavy metals, and pharmaceuticals from waste water and soil.[3,9–14]

Previous studies have focused on bulk properties of soil after treatment with BC, rather than focusing on the behavior of individual metabolites. These properties – pH, adsorption, nitrogen content, etc. – can change how organisms grow in BC-treated soil. For example, addition of BC to soil can alter metal mobility, either positively or negatively, depending on its influence on soil pH and dissolved organic matter.[3,11,13] BC adsorptive properties also improve soil physical and chemical properties by increasing pH, aeration, and water holding capacity.[1,3,15–16] Moreover, BC has been shown to restore nutrients derived from feedstock by modulating cation exchange capacity (CEC), increasing specific surface area, and influencing hydrophobicity.[10–11,17]

Physical and chemical properties of BC increase net nitrogen mineralization, increase nitrification, and enhance denitrification during microbial-mediated transformation of nutrients in soil.[11,18] Microbial activity itself is influenced by BC treatment. This has been linked to nutrient and pH changes, as well as nitrogen transformations.[10,15] BC-treated soil can also influence microbial composition by enhancing plant growth and mineralization of the soil's organic carbon.[11,15] While it is clear that BC can dramatically influence organisms in the soil by altering soil properties, much less is known about how BC influences microbial metabolism. Presumably, biochar's metabolic influence favors organisms that prefer basic growing conditions or disfavors organisms that prefer acidic growing conditions, as the populations of organisms change with the addition of BC into the soil.[11,15] BC is also effective in controlling foliar and soil-borne pathogens, as well as showing a neutral or negative effect on plant pathogens.[4–5,11,16]

Understanding the metabolomics of soil microorganisms promises to enhance our knowledge on BC's influence in the microbial community. Metabolomics is the study of small molecules that make up a network of metabolic pathways, and it provides key insights into gene-environment interactions.[19–20] Mass spectrometry (MS) and NMR techniques have been used extensively to study metabolomics. In the metabolomics field, MS is commonly used because of its high sensitivity, detection of many metabolites in a single measurement, and reliable metabolite identification through tandem mass analysis; however, MS is destructive to samples and the identities for a major fraction of detected metabolites are frequently not known.[21] NMR spectroscopy is a useful tool to quantify the extracellular metabolites, since it is non-destructive, highly reproducible, and provides a snapshot of what is occurring in the sample.[21–27] The extracellular metabolites in the media were monitored to determine the uptake of nutrients, such as glucose, adenine, and asparagine, as well as the accumulation of fermentation products and other metabolites secreted by the bacteria.[22–24,26–27] This approach has the advantage of directly monitoring nutrients in the environment. NMR spectroscopy monitors and quantifies the more abundant compounds present in biological fluids and cell extracts, and it has the advantage that it can detect metabolites that are difficult to ionize by MS.[21,28–30]

Additionally, a 1D proton NMR spectrum is often sufficient for resolving the components of a complex mixture with little overlap of the constituent compounds.[31] The detected signals can also be directly analyzed by statistical tools to identify different subgroups (i.e. healthy vs. diseased, untreated media vs. treated media, etc.), eliminating the need to identify the chemical components of the sample.[32] Alternatively, other statistical tools, like principal component analysis (PCA),[33] can be used to identify chemical differences when individual compounds are being investigated. Thus, NMR-based metabolomics is a mature and useful approach for understanding the behavior of bacteria in the presence of BC.

In this study, we treated RPMI, a complex, well-defined bacterial growth media, with BC and AC and compared how *E. coli* grew in treated media versus untreated media. While primarily useful as a model organism, *E. coli* survives readily in soil[34] and is associated with fertilization of crops.[35] We hypothesized that BC and AC would have similar effects on bacterial growth compared to untreated RPMI media. In addition to comparing the different metabolomic profiles, statistical analysis was used to highlight differences and similarities between the media types, and the overall effect on bacterial growth rates was measured. BC and AC surfaces were characterized to interpret the difference in the cell growth rates. Our results provide insight on how BC can support the development of microbiota, and they reveal a mechanism by which BC can influence microbial populations in the soil.

MATERIALS AND METHODS

Treatment of Media and Bacterial Preparation

E. coli (BL21(DE3) with an ampicillin-resistance gene) was grown in RPMI 1640 medium with L-glutamine (Fisher Scientific, Pittsburgh, USA) for the overnight stock culture and bacterial growth. Biochar Supreme, LLC (Everson, WA), generously provided Douglas fir, Ultra-Rinsed Black Owl Biochar (BC). To prepare this char, auger-fed, Douglas fir wood chips were placed into an air-fed updraft gasifier at 900–1000 °C for 1–10 s.[36–37] The

particles were collected and washed with water several times to remove fine particulates and impurities before drying at room temperature.[36–37] The biochar was sieved to a particulate size of 75–150 μm. This char has been characterized extensively in previous studies,[36–38] and our observations of point of zero charge (PZC), scanning electron microscopy (SEM), and surface porosity were consistent with these prior investigations. This confirms that the biochar used was consistent between separate batches of starting material.

Cultures were inoculated from a fresh plate of Luria-Bertani (LB) media, plus 100 μg/mL ampicillin. The overnight stock culture was shaken for 12 h at 200 rpm at 37 °C. The final optical density (O.D.) (Nanodrop One/One[c], ThermoFisher Scientific, Pittsburgh, USA) of the overnight stock culture at 600 nm was 0.855. The $O.D._{600}$ was measured to assess the rate of bacterial growth for the overnight stock culture, BC- or AC-treated media, and untreated RPMI media. 5% (by weight, 1.25 g) BC or 5% (1.25 g) Noritz Activated Carbon (AC) was added to 25 mL of RPMI media. The overnight stock culture was then divided equally into the three different media (RPMI, BC, and AC media) to begin bacterial growth. In this set of experiments, bacteria grew in the presence of BC, AC, or untreated RPMI media throughout the time course (24 h) of each experiment.

An additional set of experiments were performed where BC or AC was removed from media before inoculation (Method S1). For these experiments, 10% (by weight, 3.0 g) BC or 10% (by weight, 3.0 g) AC was added to 30 mL RPMI media. The weight-by-mass percentage was doubled (from 5 to 10%) to allow more of the media to adsorb to the particles before filtering BC or AC from RPMI media. Doubling the weight-by-mass percentage did not alter the growth rate of *E. coli,* as both growth rates for treated media were similar between the two experiments. The media was placed in a floor shaker (Innova 43 Incubator Shaker Series, New Brunswick Scientific, Edison, NJ) at 200 rpm at 25.0 °C for 24 h. This allowed ample time for BC and AC to adsorb metabolites from the media in the absence of bacterial growth. During this time, no significant growth was observed based on O.D. measurements. After 24 h of shaking, the media was filtered through a 25 mm polyethersulfone (PES), 0.2 μm sterile syringe filter. The pH for each media was measured and adjusted to have a starting pH of 7.5. The overnight stock culture was divided equally into the three filtered media to begin the bacterial growth, and experiments were performed as those described above.

Bacterial Growth

To begin the bacterial growth, the overnight stock culture was diluted into the media. From the 50 mL overnight stock culture, 15 mL each was transferred into separate flasks: one containing 1.25 g of BC in 25 mL RPMI media, one containing 1.25 g of AC in 25 mL RPMI media, and a control sample of 25 mL RPMI with no treatment. The flasks were swirled to mix BC and AC into the media. For the filter experiments, 15 mL of the 50 mL overnight stock culture was transferred into the separate flasks similarly described for the unfiltered experiments. In addition, 2 mL of media was transferred to a sterile microcentrifuge tube to represent the sample before treatment. The media was returned to the shaker to continue incubation. The average starting $O.D._{600}$ value for each flask was 0.285.

An aliquot of each sample was taken every 30 min for the first 3 h, every 3 h for the next 9 h, and the final aliquot was taken at 24 h. For each time point, 2 mL of sample was transferred to sterile microcentrifuge tubes. All samples were placed on ice to slow the bacterial growth allowing BC and AC to settle. After 5 min on ice, most of BC and AC had sedimented to the bottom of the tube so that 300 μL of the sample could be carefully transferred to a second sterile microcentrifuge tube. The sample was then diluted with 700 μL of filtered RPMI media to allow for $O.D._{600}$ measurements in the 0.1 to 1.0 range. This was necessary to prevent BC and AC from interfering with measurements of optical density. The sample was carefully mixed using the pipette tip and then transferred to a 1 cm cuvette. The $O.D._{600}$ was measured for each time point to monitor the bacterial growth.

NMR Sample Preparation

The remaining aliquot after O.D. measurement for each sample was centrifuged at $21,000 \times$ g for 12 min in preparation for NMR spectroscopy. After centrifugation, the samples were sterile filtered and 400 μL of the supernatant was transferred to another clean, sterile microcentrifuge tube. 200 μL of 200 mM phosphate buffer at pH of 7.0 with 1.000 mM trimethylsilylpropanoic acid (TMSP) in 50% D_2O was added to the supernatant as the internal NMR reference and lock solvent. For NMR analysis, 550 μL of the sample was transferred to a clean 5 mm NMR tube (Wilmad Lab Glass, USA).

NMR Spectroscopy

The ^1H NMR spectra were obtained at 600 MHz and at a temperature of 298 K on a 600 MHz Bruker Avance III cryoprobe-equipped NMR spectrometer. A 1D-NOESY (noesypr1d) pulse sequence was used to obtain the spectra. The pulse sequence used presaturation on the water signal during the 4 s relaxation delay (d1) and the 50 ms mixing time (d8) to suppress the water signal at 4.75 ppm (o1p). A total of 64 free induction decays (FIDs) were collected with a 20 ppm spectral width. The TMSP reference peak was used as an internal standard.

The TMSP peak for each spectrum was calibrated to 0 ppm and then peaks were manually phased and baseline corrected. Compounds in the processed spectra were identified and quantified using AMIX-Viewer v3.9.14 software (Bruker Biospin GmbH). Peaks were identified by comparison to a library of pure, 3.000 mM standard compounds. In addition to serving as a chemical shift reference, the TMSP peak was also used as an analytical standard. The library was created in-house, and it contained a total of 56 common metabolites. These metabolites were not targeted to a specific pathway, but instead were chosen to focus on glycolysis, the tricarboxylic acid cycle, and soluble amino acids. The library contained chemical shift data and peak integrations for each compound, although some peaks in crowded spectral regions were excluded from analysis. The output from AMIX was a listing of concentrations for each of the 56 compounds at a given time point. Concentrations versus time were collected to form a large data matrix for AC-treated, BC-treated, or untreated RPMI media, and this matrix was then used for statistical analysis, described below.

BET and SEM Analysis

The Brunauer-Emmett-Teller (BET) analysis was used to measure the adsorption of nitrogen gas on the surface area of BC and AC. BET surface areas, pore volumes, and averaged pore diameters of BC and AC were examined on a Micromeritics TriStar II Plus 3030 surface area analyzer using a nitrogen adsorption isotherm at 77 K.

Scanning electron microscopy (SEM) was used to determine BC and AC morphology. Sample preparation for SEM was prepared as described above, however, reagent amounts and volumes were scaled down for microscopy. 150 mg of BC or AC was added to 3 mL RPMI media in a sterile 15 mL conical tube. This set of samples was placed in the shaker for 24 h with no bacteria to characterize BC and AC morphologies in RPMI media alone. The 10 mL overnight stock culture had a final O.D.$_{600}$ of 0.732. 500 mg of BC or AC was added to 10 mL RPMI media and then the overnight culture was equally divided into the three media types. The starting O.D.$_{600}$ value for each media was 0.224. The O.D.$_{600}$ after 24 h of growing was 0.815 for RPMI media, 0.668 for BC-treated media, and 0.375 for AC-treated media. Each sample was vacuum filtered using a Buchner funnel. The samples were each placed into a sterile glass vial and dried in the oven for three days at 67 °C. To analyze the samples on SEM, carbon tape was placed onto a specimen holder, and the tape was gently coated with an even layer of BC or AC. Excess particles were removed using compressed air. Once all samples were mounted onto the specimen holder, the holder was placed under vacuum and coated with 20 nm of Pt in a sputter coater. The surface morphologies of BC and AC were then examined by SEM using a JEOL JSM-6500F FE-SEM at 5 kV.

Statistical Analysis

Statistical analysis was conducted using MetaboAnalyst.[39] The average metabolite concentrations of three replicates for each sample was determined for each incubation time and media type. MetaboAnalyst normalized the data with Pareto scaling, which is mean centered and divided by the square root of the standard deviation of each variable. Pareto scaling was used to reduce the influence of the intense peaks and emphasize the weaker peaks to interpret the biological relevance.[33] Once the data were normalized, multivariate analysis (PCA) and cluster analysis (heatmaps) were used to perform data analysis.

For PCA analysis, the data set was divided into principal components (PCs) to identify the statistical differences between the classes. The first component (PC1) was the linear combination of the original predictor variables that captured the maximum variance in the data, whereas the other components (second, third, fourth, etc.) were the linear combination that captured the remaining variance in the data set and were orthogonal to the first component.[40–41] A biplot was used to identify metabolites that were significantly different between RPMI, BC, and AC samples.[42] The metabolites with the largest variance were easily identified in the biplot due to a larger vector magnitude. Significant metabolites ($p < 0.05$) were determined using a two-sample t-test with unequal variances. The metabolites identified as statistically significant were colored yellow in the biplot; insignificant metabolites were colored gray.

A heatmap of normalized, relative concentrations was used to visualize the relationship between two sets of data by using a color scale.[43] The heatmap employed a hierarchical clustering analysis of the metabolites that was based on Pearson's correlation and Ward's linkage. Pearson's correlation determined the linear correlation between the variables and Ward's linkage algorithm was based on the Euclidean distance that minimized the sum of the squares of any two clusters.[39,44–45] The heatmap used a color scale to represent the variance in concentration for each metabolite in the sample.

RESULTS AND DISCUSSION

Initial Adsorption of Metabolic Compounds

The adsorptive properties of BC and AC make them ideal as soil additives in agriculture because BC and AC enhance the soil's physical and chemical properties by increasing the water holding capacity, retaining nutrients, enhancing CEC, increasing surface area, and influencing hydrophobicity.[1,3,10,15] Variations in BC and AC feedstock and pyrolysis conditions produce materials with varied adsorptive properties. This allows chars to be tailored to enhance specific soil conditions. Varying the adsorptive properties of BC is an effective strategy for removing specific chemicals in soil and water. Woody chars typically have a higher CEC, allowing them to be used as a carbon sequestration agent as well as a soil amendment.[46–47] Woody BCs are typically used to remove metals, pesticides, and pharmaceuticals from soil and water.[46,48–50]

Both organic and inorganic BC components influence adsorption.[51] Chars that contain a higher percentage of ash and low carbon content are not as energy efficient and are less useful for adsorbing compounds.[47] BC and AC containing a higher carbon content, usually found in woody and plant materials, demonstrates an increased adsorption of water, metals, and metabolites relative to chars containing a lower carbon content.[47] High pyrolysis temperatures effect the sorption of BC by increasing the surface area, microporosity, and hydrophobicity, whereas the low pyrolysis temperatures removes inorganic and polar organic contaminants by oxygen-containing functional groups, electrostatic attraction, and precipitation.[48] In this study, we used Ultra-Rinsed Black Owl Biochar, a commercially available soil amendment manufactured from Douglas fir waste wood.

Both BC and AC adsorbed many metabolites when introduced into RPMI media (Figure 1) including amino acids and D-glucose. Figure 1 represents a few of the amino acids that were adsorbed by BC and AC that are not part of the tricarboxylic acid (TCA) cycle. One-way ANOVA was used to identify significant amino acids that were adsorbed after initial treatment with BC or AC. Five amino acids (L-leucine, L-lysine, L-proline, L-phenylalanine, and L-tyrosine) were strongly adsorbed by AC and BC ($p < 0.005$), suggesting a significant interaction with these compounds. L-isoleucine, L-methionine, and L-serine were less significant ($p < 0.05$) but still strongly adsorbed. Other amino acids, including L-lysine, and cis-4-hydroxy-L-proline, showed a decrease in concentration but were not statistically significant. Overall, the addition of BC and AC into the RPMI media introduced an environmental factor that altered the bacterial growth rate (Figure 2).

E. coli Growth in RPMI vs. Treated Media

E. coli was grown in RPMI media for the overnight stock culture up to 12 h and used as the starting culture with an initial $O.D._{600}$ of 0.285. RPMI media was treated with BC and AC to observe how their presence affected the bacterial growth rate. In unfiltered experiments, BC and AC remained in RPMI media during bacterial growth. In filtered experiments, BC and AC were filtered from RPMI media before bacterial growth. From the $O.D._{600}$, it was observed that *E. coli* grew more readily in RPMI media with more abundant metabolites than treated RPMI media, likely indicating the adsorption of nutrients by BC and AC influenced the bacterial growth rate (Figure 2). For the first 3 h, BC- and AC-treated media had a similar growth rate, whereas after 3 h *E. coli* adapted to BC-treated media and reached stationary phase for unfiltered AC-treated media (Figure 2A). The stationary phase for both RPMI and unfiltered BC-treated media was reached around 6 h. The filtered BC- and AC-treated media showed qualitatively similar results as unfiltered media, although the initial $O.D._{600}$ values were slightly noisier when media was filtered. In the filtered experiments, AC reached stationary phase faster than BC (Figure 2B), but the trend in final $O.D._{600}$ values was identical to the unfiltered experiments. The slower growth rate seen in BC and AC was from the adsorption of metabolites that were needed for bacterial growth. For example, the starting concentration of D-glucose decreased when BC and AC were introduced into RPMI media. Furthermore, L-asparagine and L-glutamine also had a significant decrease in concentration once BC and AC were introduced into RPMI media.

Bacterial Interaction with BC and AC Particles

After confirming the effects of AC and BC on bacterial growth, we investigated the structural interaction of bacterial cells with BC and AC surfaces using scanning electron microscopy (SEM). SEM was used to measure the surface morphology of BC and AC without RPMI media, with RPMI media, and with *E. coli* in RPMI media. The surface of BC was observed to be flat and smooth, while AC was porous and coarse (Figure 3 and Figure S1), agreeing with previous comparisons of AC and BC.[36–37] SEM images of BC showed a morphology change as RPMI and *E. coli* were introduced to the char, with the smoother microscopic texture of BC making it easier to observe the attachment of material to the surface (Figure 3A and Figure S1). When BC was introduced to RPMI media and *E. coli* cultures, there were small patches of adsorbed metabolites and bacterial cells visible on the surface of the char (Figure 3B and 3C). After treatment with bacteria, the biochar appeared to have numerous bacterial colonies (Figure 3C), and several of these colonies contained clusters of 3–4 1 μm sized cells. *E. coli* biofilms can take up to several days to form,[52] but Sugimoto, *et al.* observed similarly sized clusters during the early formation of *E. coli* biofilms.[53] This suggests that biofilms may form on the flat surfaces present in biochar. The formation of biofilms are due to bacterial cells producing an extracellular polymeric matrix comprising of polysaccharides, proteins, lipids, and nucleic acids.[54] Each of these components would likely enhance attachment to charred biomass, which is known to contain not only hydrophobic interacting surfaces,[55] but also hydrogen bond donors/acceptors,[55] and ionizable groups.[56] Importantly, most of these chemical features differ significantly in AC, which may make it less amenable to bacterial attachment.[54] The physical basis of surface attachment is influenced by many factors, including electrostatics

and metal ion content,[57] and further studies are needed to understand why bacteria attach to some surfaces and not others.

On the other hand, the coarse surface of AC made it difficult to observe any adsorbed metabolites or bacteria (Figure 3, D-F). AC was observed to have a larger surface area than BC (Figure 3), and overall adsorption of metabolites was found to be higher (Figure 1). The absence of bacterial clusters, however, suggests that biofilms will form much more slowly on the surface of AC, if at all. The adsorption of metabolites on BC and AC introduced an environmental stress to the media, where bacteria had to compete for nutrients (Figure 2). It is possible that this stress factor significantly altered the bacterial growth, making biofilm formation more likely on BC surfaces than AC surfaces. As noted above, the surface charge of BC and AC strongly influences the adsorption of metabolites and bacteria.[54,57] Measurement of the point of zero charge (PZC) revealed that BC had a higher PZC than AC (pH 9.793 ± 0.005 vs pH 8.920 ± 0.003, Figure S2 and Method S2). The higher PZC for BC likely enhances the capacity to adsorb charged species by favoring electrostatic interactions with metabolites and cell surface components at neutral pH, where our studies were performed.[57]

The pore size of BC and AC can potentially modulate adhesion of bacteria to the material. Previous studies have suggested a relationship between pore size and bacterial adhesion. An overly large or small pore size will diminish adhesion due to pore curvature being too small for the bacteria to adhere (large pore size) or due to physical exclusion from the pores (small pore size).[11] Brunauer, Emmett, and Teller (BET) analysis was used to estimate the surface area and average pore size of BC and AC. This analysis does not quantify surface curvature, but rather measures the surface areas of solids by physical adsorption of N_2 gas molecules.

BET analysis revealed that BC had a smaller average pore size than AC (15.0 ± 0.1 Å vs. 16.1 ± 0.6 Å, respectively; Table 1). Moreover, AC has a higher surface area than the BC used in this study. These observations are consistent with the fact that AC is able to adsorb more small compounds overall, suggesting that surface area and adsorption capacity play the primary role in modulating bacterial growth following treatment with BC or AC. Surface area and pore size may also play a secondary role in controlling bacterial attachment, even though the BET pore sizes are much smaller than even a single bacterial cell. This secondary role follows because the BET pore size will influence which cell surface components of the *E. coli* outer membrane are able to interact with the BC or AC surface. Additionally, it is known that selective adsorption of nutrients themselves are able to assist in bacterial accumulation to a surface.[58] Therefore, the surface characteristics of BC and AC on a molecular scale can potentially have a larger-scale influence on bacterial colonization. While it is difficult to correlate BET measurements with surface roughness,[59] the BET surface area approximately reflects the smoothness of the surface as visualized by SEM (Figure 3 A-C). Thus, it is possible that pore size in BC is more conducive to binding *E. coli* cell surface components. This would in turn make the smooth, flat surfaces of BC more easily able to accommodate bacterial attachment and colonization. Additionally, the BC used in this study is prepared by pyrolysis of wet bio-mass. This treatment is thought to increase surface area as pockets of steam and other volatiles rupture during pyrolysis.[36–38,46,50] It is possible that this wet pyrolysis treatment also plays a role in bacterial attachment.

Metabolite Excretion and Adsorption During Bacterial Growth

To investigate the effect BC and AC have on glucose metabolism, we examined the concentration dependence of several key compounds in glycolysis and the TCA cycle. The TCA cycle is a good indicator of bacterial growth in the presence of external stressors, because it represents the major pathways for energy flux in the cell.[60–61] D-glucose is one of the main carbon sources in RPMI media that was depleted and was shown to have an inverse-relationship with bacterial growth (Figure 2). The process of glycolysis rapidly converts D-glucose to pyruvate in *E. coli*, and both compounds can be quantified using NMR (Figure 4).[23] D-glucose was completely depleted in RPMI and BC-treated media (an indication of bacterial growth), whereas the concentration of D-glucose in AC-treated media was only slightly reduced (minimal bacterial growth). When D-glucose is depleted as part of the TCA cycle, the concentration of byproducts, like acetate and pyruvate increase.

Examination of the TCA cycle revealed several similarities and differences between cells treated with AC or BC (Figure 4). For example, acetoin, lactate, and L-valine showed a decrease in concentration for BC- and AC-treated media, whereas RPMI media had a higher concentration than treated media for these compounds. The citrate concentration in BC- and AC-treated media was fairly constant during the experiment, whereas in RPMI media the concentration of citrate increased over the same time frame. L-glutamine, D-glucose, and L-asparagine decreased slowly in concentration for BC-treated media and RPMI media, whereas in AC-treated media the concentrations for these metabolites decreased more quickly. In the TCA cycle, 2-oxoglutarate for BC-treated media had a similar behavior compared to RPMI media. Fumarate, L-aspartate, L-glutamate, and acetate for BC-treated media behaved differently compared to AC-treated and RPMI media. The patches of adsorbed metabolites on the surface of BC and AC seen in the SEM images may explain why we observed a difference in concentrations for a few metabolites in RPMI media (Figures 3 and 4).

The concentration of the extracellular metabolites was also visualized using a clustered heatmap (Figure 5, Figure S3, and Figure S5C). A heatmap graphically represents the change in metabolite concentrations versus time with a color scale being used to represent the row Z-score. This heatmap covers the complete list of 56 metabolites used in this analysis, including the glycolysis-related compounds already discussed.

In general, AC-treated media had very low concentrations for most of the metabolites in comparison to BC-treated and RPMI media. AC adsorbed more metabolites than BC, as evidenced from the first time point (0 h) before the cultures were inoculated. Interestingly, adsorption profiles for AC and BC differ significantly, with compounds like L-isoleucine, choline chloride, L-leucine, and 2-oxoglutarate adsorbing more strongly to AC. Over time, however, the metabolic profiles for BC- and AC-treated media were seen to be similar when compared to untreated RPMI media. For example, glycine and L-asparagine in BC- and AC-treated media had very similar trends in decreasing concentration compared to untreated RPMI media.

Several compounds, including acetate, L-glutamate, L-proline, L-alanine, and pyruvate, peaked in concentration in RPMI media at 6 h. After this, they rapidly decreased as key

metabolites, including D-glucose (a carbon source) and L-glutamine (a nitrogen source), were utilized by *E. coli* cells. Given that cells replicate more rapidly in RPMI media, this peak may reflect the point at which the initial nutrients are depleted, and cells must adapt to a more competitive environment. In AC- and BC-treated media, the overall nutrient concentrations are already reduced, and this effect becomes less pronounced. It is weakly visible in BC-treated media, but such an effect is not observed in AC-treated samples.

The heatmap clusters into two general classes of compounds: those that increase in concentration in RPMI media, and those that decrease over time. Smaller clusters reflect differences in behavior of those compounds in AC- and BC-treated media. Across all three types of media, the concentrations were generally observed to correlate, although several exceptions to this were observed. The increasing concentration of fumarate in BC-treated media, already discussed above, is one example of this. The increase of formate and ethanolamine in AC-treated media at longer time points is another. For these two compounds the concentration remains approximately constant in BC-treated media, and in RPMI the concentration is observed to decrease. It is not clear why these compounds behave differently in media treated with AC. Importantly, the compounds do not appear to form clusters based on simple chemical properties such as charge and/or hydrophobicity: this suggests that the concentration dependence originates from changes in bacterial behavior and not selective surface interactions. To investigate chemical trends among metabolites, compounds in the heatmap (Figure 5) were rearranged based on their chemical properties. Amino acids, vitamins, sugars, constituent bases, and nucleosides were grouped in an alternative organization of the heatmap (Figure S3). No significant trends were observed within each group, suggesting that the concentration dependence arises due to metabolic changes and not the adsorptive properties of AC or BC, which should be similar for similar compounds. This hypothesis is further supported by experiments with filtered media, as described below.

Analysis of the initial adsorption of metabolites revealed that both BC and AC depleted some nutrients needed for bacterial growth. Overall, BC adsorbed a lower quantity of metabolites than AC. The filtered and unfiltered media had similar characteristics in metabolite adsorptions. PCA analysis had very similar results for unfiltered and filtered media, where BC-treated media had similar characteristics to AC-treated and RPMI media (Figure 6 and Figure S5). The heatmaps overall had similar metabolic profiles between filtered and unfiltered media (Figure 5 and Figure S5). For unfiltered samples, the adsorbed metabolites can potentially be returned to the media, leading to persistent differences through the growth cycle. However, filtration removes AC or BC, and those samples permanently lose the initial concentration of adsorbed metabolites.

Since filtered and unfiltered samples both have similar profiles, the desorption and resorption of metabolites to the surface during the experiment do not appear to alter the bacteria growth significantly. Rather, it is the initial adsorption of metabolites to the char's surface that seems to most dramatically influence the bacterial growth rate. This is significant, as it suggests that supplementing BC with several key nutrients may be an effective strategy for offsetting any adverse effects in soil bacterial growth rates.

Statistical Analysis of Metabolites Present After Growth

The metabolic data were further analyzed using statistical analysis provided by the MetaboAnalyst suite.[39] PCA was used to determine statistically meaningful differences between three media types (score plot shown in Figure 6A and Figure S5A). Removal of BC or AC by filtration before inoculation made essentially no difference in the principal components (Figure 6A). Both filtered and unfiltered growth showed a clear differentiation between RPMI and AC-treated media as determined by the ellipses representing 95% confidence intervals (Figure 6A and Figure S5A). However, the behavior of BC-treated media showed similarities to both AC-treated and RPMI media, demonstrated by its overlap on the scatter plot.

The first and second component for unfiltered and filtered media accounted for the largest variation between the media. These two components combined account for 88.3% of the variance in the data, with the first two components (PC1 and PC2) accounting for 55.6% and 32.7% of the variance, respectively. This observation that BC-treated media retains characteristics of AC-treated media as well as untreated RPMI media is consistent with qualitative comparisons previously noted above. Since AC adsorbs more metabolites than BC, AC can be viewed as a more aggressive amendment, whereas BC retains some of the adsorptive capabilities of AC while promoting conditions favorable for bacterial growth.

An examination of the scatter plot (and biplot) reveals that the early time points of BC-treated media cluster near RPMI media, whereas later time points cluster with AC-treated media. After approximately 6 h, the data points corresponding to BC-treated media diverge from the cluster of early timepoints on the scatter plot and trend toward the cluster of AC-treated media. It is this multi-modal behavior that gives rise to a substantially larger confidence interval for BC-treated media (Figure 6A and Figure S5A). Based on the loadings (Figure 6B and Figure S5B), D-glucose, L-arginine, and acetate contribute significantly to the second principal component, and the depletion of these compounds leads to the transition from one cluster to the other on the biplot.

The component loadings identify which metabolite concentration differences contribute to PC1 and PC2 (Figure 6B and Figure S5B).[39] The metabolites with the largest variance in the metabolic profile were identified and labeled as significant metabolites (yellow dots, Figure 6B and Figure S5B). The magnitude of the vectors for the significant metabolites quantifies the change in the concentrations over time for each principal component. Therefore, the longer vectors represent a larger relative change in metabolite concentrations and the shorter vectors represent a smaller change in metabolite concentrations. These largest contributors are the metabolites that deviate in behavior from the insignificant metabolites, which are clustered near the origin of the loading plot (Figure 6B, gray dots). The size of each metabolite's loading is based on its trend during the growth. For example, D-Glucose decreased in concentration over time, while acetate increased in concentration, resulting in these metabolites being on opposite ends of Loading 1 and Loading 2 (Figure S4). The largest contributors to the first loading were acetate, L-arginine, isoamyl isovalerate, and D-glucose, whereas the second loading was dominated by acetate, D-glucose and L-arginine. These data indicate that, following treatment with BC or AC, significant differences are observed in the extracellular metabolite concentrations of these compounds. BC and AC

alter the media in complex ways, leading to significant differences in several extracellular metabolite concentrations, and these changes cannot be explained by the adsorption of simply one or two compounds. Moreover, some metabolite concentrations remain unaffected or show little discriminatory power between samples (Figure 6B, grey circles). This suggests that, treatment with AC and BC leaves many compounds unaffected during bacterial growth.

To summarize, based on our measurements, there were statistically significant differences between RPMI and AC-treated media, whereas BC-treated media shared characteristics with both RPMI and AC-treated media. This suggests that the favorable properties of BC, namely, its ability to retain nutrients, may not adversely affect the bacterial life cycle in the way that other adsorbents, such as AC, might. This is especially true at early time points, where extracellular metabolite concentrations for BC-treated cells were observed to behave similarly to cells growing in untreated media. Together, these results have implications for biochar when used as a soil amendment. BC's adsorption properties enhance soil fertility and structure, add needed nutrients like carbon and nitrogen to the soil, and enhance soil microorganisms [4–7]. Moreover, BC allows crops to grow larger and faster because BC enhances the soil's physical and chemical properties by increasing pH, aeration, water holding capacity, and adding nutrients; BC also adsorbs metabolites that alter bacterial growth.[3,11,13]

This study begins to explain these effects at the level of the bacterial metabolome. Here, the behavior of metabolites demonstrates that BC can effectively adsorb certain compounds, similar to AC, while leaving others available for utilization by soil microbiota. It is this property that allows BC to exhibit the favorable properties of RPMI media during the early time points when bacteria are doubling rapidly. At the same time, BC is known to adsorb hydrophobic compounds and retain nitrogenous fertilizers,[11–13] making conditions favorable for plant growth. Combined, these properties create conditions that favor growth of both crops and soil microbiota. While BC can adsorb nutrients needed by microorganisms, as demonstrated by the initial depletion of D-glucose, oxoglutarate, and several other compounds, this effect appears to be minor compared to AC, where aggressive adsorption of these compounds leads to poor bacterial growth. Interestingly, the selective adsorption of metabolites could lead to conditions that favor one particular organism over another. While we have not explored the influence of BC on different populations of microbes, this work strongly suggests that BC can alter metabolite concentrations to favor one particular organism over another. For example, the addition of BC or AC mainly had a positive effect on the abundance of mycorrhizal fungi, but in some cases BC or AC limited the nutrients and the mycorrhizal fungi was hindered.[62] It was also observed that the relationship between mycorrhizal fungi and BC sequesters carbon (mitigating climate change) to restore the ecosystem.[62]

In summary, as a soil amendment, biochar's metabolic effects on soil microbiota have been largely uninvestigated. Here, we explored how biochar can alter the metabolomic profile of *E. coli.* There were significant differences between RPMI and AC-treated media, whereas BC-treated media shared characteristics with both RPMI and AC-treated media. This suggests a mechanism whereby BC can adsorb nutrients without adversely affecting soil microbiota. While cell culture does not represent soil conditions, the experiments capture the

essential properties of adsorption by BC and AC, evidenced by the concentration of metabolites. Efforts are underway to understand how BC influences the populations of soil biota.

Supplementary Material

Refer to Web version on PubMed Central for supplementary material.

ACKNOWLEDGMENT

ABBREVIATIONS

AC	Activated Carbon
BC	Biochar
NMR	Nuclear Magnetic Resonance
TCA	Tricarboxylic acid
PCA	Principal Component Analysis
CEC	cation exchange capacity
LB	Luria-Bertani
PES	polyethersulfone
TMSP	trimethylsilypropanoic acid
FIDs	free induction decays
BET	Brunauer-Emmett-Teller
SEM	scanning electron microscopy

REFERENCES

1. Akhter A; Hage-Ahmed K; Soja G; Steinkellner S Compost and Biochar Alter Mycorrhization, Tomato Root Exudation, and Development of *Fusarium Oxysporum* F. Sp. Lycopersici. Front. Plant Sci 2015, 6, 529. [PubMed: 26217373]
2. Das O; Sarmah AK; Zujovic Z; Bhattacharyya D Characterisation of Waste Derived Biochar Added Biocomposites: Chemical and Thermal Modification. Sci. Total Environ 2016, 550, 133–142. [PubMed: 26808404]

3. Sun CX; Chen X; Cao MM; Li MQ; Zhang YL Growth and Metabolic Responses of Maize Roots to Straw Biochar Application at Different Rates. Plant Soil 2017, 416 (1–2), 487–502.

4. Copley TR; Aliferis KA; Jabaji S Maple Bark Biochar Affects Rhizoctonia Solani Metabolism and Increases Damping-Off Severity. Phytopathology 2015, 105, 1334–1346. [PubMed: 25938176]

5. French E; Iyer-Pascuzzi AS A Role for the Gibberellin Pathway in Biochar-Mediated Growth Promotion. Sci. Rep 2018, 8 (1), 5389. [PubMed: 29599525]

6. Khodadad CLM; Zimmerman AR; Green SJ; Uthandi S; Foster JS Taxa-Specific Changes in Soil Microbial Community Composition Induced by Pyrogenic Carbon Amendments. Soil Biol. Biochem 2011, 43, 385–392.

7. Kolton M; Harel YM; Pasternak Z; Graber ER; Elad Y; Cytryn E Impact of Biochar Application to Soil on the Root-Associated Bacterial Community Structure of Fully Developed Greenhouse Pepper Plants. Appl. Environ. Microbiol 2011, 77, 4924–4930. [PubMed: 21622786]

8. Lehmann J; Gaunt J; Rondon M Bio-Char Sequestration in Terrestrial Ecosystems - a Review. Mitigation and Adaptation Strategies for Global Change 2006, 11, 403–427.

9. Lieke T; Zhang X; Steinberg CEW; Pan B Overlooked Risks of Biochars: Persistent Free Radicals Trigger Neurotoxicity in *Caenorhabditis elegans*. Environ. Sci. Technol 2018, 52 (14), 7981–7987. [PubMed: 29916700]

10. Keiblinger KM; Liu D; Mentler A; Zehetner F; Zechmeister-Boltenstern S Biochar Application Reduces Protein Sorption in Soil. Org. Geochem 2015, 87, 21–24.

11. Lehmann J; Rillig MC; Thies J; Masiello CA; Hockaday WC; Crowley D Biochar Effects on Soil Biota - a Review. Soil Biol. Biochem 2011, 43, 1812–1836.

12. Taha SM; Amer ME; Elmarsafy AE; Elkady MY Adsorption of 15 Different Pesticides on Untreated and Phosphoric Acid Treated Biochar and Charcoal from Water. J. Env. Chem. Eng 2014, 2 (4), 2013–2025.

13. Venegas A; Rigol A; Vidal M Viability of Organic Wastes and Biochars as Amendments for the Remediation of Heavy Metal-Contaminated Soils. Chemosphere 2015, 119, 190–198. [PubMed: 24995385]

14. Yang Y; Sheng G Pesticide Adsorptivity of Aged Particulate Matter Arising from Crop Residue Burns. J. Agric. Food. Chem 2003, 51, 5047–5051. [PubMed: 12903968]

15. Zheng J; Chen J; Pan G; Liu X; Zhang X; Li L; Bian R; Cheng K; Jinwei Z Biochar Decreased Microbial Metabolic Quotient and Shifted Community Composition Four Years after a Single Incorporation in a Slightly Acid Rice Paddy from Southwest China. Sci. Total Environ 2016, 571, 206–217. [PubMed: 27471985]

16. Waqas M; Shahzad R; Hamayun M; Asaf S; Khan AL; Kang S-M; Yun S; Kim K-M; Lee I-J Biochar Amendment Changes Jasmonic Acid Levels in Two Rice Varieties and Alters Their Resistance to Herbivory. PloS one 2018, 13 (1), e0191296–e0191296. [PubMed: 29373575]

17. Xiao X; Chen B; Chen Z; Zhu L; Schnoor JL Insight into Multiple and Multilevel Structures of Biochars and Their Potential Environmental Applications: A Critical Review. Environ. Sci. Technol 2018, 52 (9), 5027–5047. [PubMed: 29634904]

18. Zhang H; Voroney RP; Price GW Effects of Temperature and Processing Conditions on Biochar Chemical Properties and Their Influence on Soil C and N Transformations. Soil Biol. Biochem 2015, 83, 19–28.

19. Bingol K; Bruschweiler-Li L; Li D; Zhang B; Xie M; Brüschweiler R Emerging New Strategies for Successful Metabolite Identification in Metabolomics. Bioanalysis 2016, 8, 557–573. [PubMed: 26915807]

20. Ravanbakhsh S; Liu P; Bjorndahl TC; Mandal R; Grant JR; Wilson M; Eisner R; Sinelnikov I; Hu X; Luchinat C; Greiner R; Wishart DS Accurate, Fully-Automated NMR Spectral Profiling for Metabolomics. PLOS ONE 2015, 10 (5), e0124219. [PubMed: 26017271]

21. Nagana Gowda GA; Raftery D Can NMR Solve Some Significant Challenges in Metabolomics? J. Magn. Reson 2015, 260, 144–160. [PubMed: 26476597]

22. Bingol K; Brüschweiler R NMR/MS Translator for the Enhanced Simultaneous Analysis of Metabolomics Mixtures by NMR Spectroscopy and Mass Spectrometry: Application to Human Urine. Journal of Proteome Research 2015, 14 (6), 2642–2648. [PubMed: 25881480]

23. Dörries K; Lalk M Metabolic Footprint Analysis Uncovers Strain Specific Overflow Metabolism and D-Isoleucine Production of Staphylococcus aureus COL and HG001. PLOS ONE 2013, 8 (12), e81500. [PubMed: 24312553]

24. Leonard A; Gierok P; Methling K; Gómez-Mejia A; Hammerschmidt S; Lalk M Metabolic Inventory of Streptococcus pneumoniae Growing in a Chemical Defined Environment. Int. J. Med. Microbiol 2018, 308 (6), 705–712. [PubMed: 29398251]

25. Somerville GA; Powers R, Growth and Preparation of Staphylococcus epidermidis for NMR Metabolomic Analysis In Staphylococcus epidermidis: Methods and Protocols, Fey PD, Ed. Humana Press: Totowa, NJ, 2014; pp 71–91.

26. Sun J-L; Zhang S-K; Chen J-Y; Han B-Z Metabolic Profiling of Staphylococcus aureus Cultivated under Aerobic and Anaerobic Conditions with 1H NMR-Based Nontargeted Analysis. Can. J. Microbiol 2012, 58 (6), 709–718. [PubMed: 22571732]

27. Zhang B; Powers R Analysis of Bacterial Biofilms Using NMR-Based Metabolomics. Future medicinal chemistry 2012, 4 (10), 1273–1306. [PubMed: 22800371]

28. Dettmer K; Aronov PA; Hammock BD Mass Spectrometry-Based Metabolomics. Mass Spectrom. Rev 2007, 26 (1), 51–78. [PubMed: 16921475]

29. Markley JL; Brüschweiler R; Edison AS; Eghbalnia HR; Powers R; Raftery D; Wishart DS The Future of NMR-Based Metabolomics. Curr. Opin. Biotechnol 2017, 43, 34–40. [PubMed: 27580257]

30. Marshall DD; Powers R Beyond the Paradigm: Combining Mass Spectrometry and Nuclear Magnetic Resonance for Metabolomics. Prog. Nucl. Magn. Reson. Spectrosc 2017, 100 (Supplement C), 1–16. [PubMed: 28552170]

31. Li DW; Wang C; Brüschweiler R Maximal Clique Method for the Automated Analysis of NMR TOCSY Spectra of Complex Mixtures. J. Biomol. NMR 2017, 68, 195–202. [PubMed: 28573376]

32. Bingol K; Brüschweiler R Knowns and Unknowns in Metabolomics Identified by Multidimensional NMR and Hybrid MS/NMR Methods. Curr. Opin. Biotechnol 2017, 43, 17–24. [PubMed: 27552705]

33. Worley B; Powers R Multivariate Analysis in Metabolomics. Curr. Metabolomics 2013, 1, 92–107. [PubMed: 26078916]

34. van Elsas JD; Semenov AV; Costa R; Trevors JT Survival of Escherichia coli in the Environment: Fundamental and Public Health Aspects. The ISME Journal 2010, 5, 173. [PubMed: 20574458]

35. HABTESELASSIE MY; BISCHOFF M; APPLEGATE B; REUHS B; TURCO RF Understanding the Role of Agricultural Practices in the Potential Colonization and Contamination by Escherichia coli in the Rhizospheres of Fresh Produce. J. Food Prot 2010, 73 (11), 2001–2009. [PubMed: 21219711]

36. Karunanayake AG; Todd OA; Crowley ML; Ricchetti LB; Pittman CU, Jr.; Anderson R; Mlsna TE Rapid Removal of Salicylic Acid, 4-Nitroaniline, Benzoic Acid and Phthalic Acid from Wastewater Using Magnetized Fast Pyrolysis Biochar from Waste Douglas Fir. Chem. Eng. J 2017, 319, 75–88.

37. Karunanayake AG; Todd OA; Crowley M; Ricchetti L; Pittman CU, Jr.; Anderson R; Mohan D; Mlsna T Lead and Cadmium Remediation Using Magnetized and Nonmagnetized Biochar from Douglas Fir. Chem. Eng. J 2018, 331, 480–491.

38. Bombuwala Dewage N; Liyanage AS; Pittman CU; Mohan D; Mlsna T Fast Nitrate and Fluoride Adsorption and Magnetic Separation from Water on A-Fe2o3 and Fe3O4 Dispersed on Douglas Fir Biochar. Bioresour. Technol 2018, 263, 258–265. [PubMed: 29753258]

39. Xia J; Wishart DS, Using Metaboanalyst 3.0 for Comprehensive Metabolomics Data Analysis In Current Protocols in Bioinformatics, John Wiley & Sons, Inc.: 2002.

40. Begam BF; Kumar JS Visualization of Chemical Space Using Principal Component Analysis. World Applied Sciences Journal 2014, 29, 53–59.

41. Jolliffe IT Principal Component Analysis. Springer-Verlag: New York, 2002.

42. Udina F Interactive Biplot Construction. J. Stat. Software 2005, 13 (5), 16.

43. Khoo M; Rozaklis L; Hall C; Kusunoki D; Rehrig M Heat Map Visualizations of Seating Patterns in an Academic Library. iConference 2014 Proceedings 2014, 612–620.

44. Miyamoto S; Suzuki S; Takumi S, Clustering in Tweets Using a Fuzzy Neighborhood Model. In WCCI 2012 IEEE World Congress on Computational Intelligence, Brisbane, Australia, 2012.

45. Strauss T; Maltitz M. J. v. Generalising Ward's Method for Use with Manhattan Distances. PLOS ONE 2017, 12 (1), 1–21.

46. Abdel-Fattah TM; Mahmoud ME; Ahmed SB; Huff MD; Lee JW; Kumar S Biochar from Woody Biomass for Removing Metal Contaminants and Carbon Sequestration. J. Ind. Eng. Chem 2015, 22, 103–109.

47. Allaire S; Lange S; Auclair I; Quinche M; Greffard L Report: Analyses of Biochar Properties.; Université Laval, Québec, Canada: Centre de Recherche sur les Matériaux Renouvelables, 2015; p 59.

48. Ahmad M; Rajapaksha AU; Lim JE; Zhang M; Bolan N; Mohan D; Vithanage M; Lee SS; Ok YS Biochar as a Sorbent for Contaminant Management in Soil and Water: A Review. Chemosphere 2014, 99, 19–33. [PubMed: 24289982]

49. Beesley L; Moreno-Jiménez E; Gomez-Eyles JL; Harris E; Robinson B; Sizmur T A Review of Biochars' Potential Role in the Remediation, Revegetation and Restoration of Contaminated Soils. Environ. Pollut 2011, 159 (12), 3269–3282. [PubMed: 21855187]

50. Mohan D; Sarswat A; Ok YS; Pittman CU, Jr. Organic and Inorganic Contaminants Removal from Water with Biochar, a Renewable, Low Cost and Sustainable Adsorbent – a Critical Review. Bioresour. Technol 2014, 160, 191–202. [PubMed: 24636918]

51. Soudek P; Rodriguez Valseca IM; Petrová Š; Song J; Van k T Characteristics of Different Types of Biochar and Effects on the Toxicity of Heavy Metals to Germinating Sorghum Seeds. Journal of Geochemical Exploration 2017, 182, 157–165.

52. Beloin C; Roux A; Ghigo JM, Escherichia coli Biofilms In Bacterial Biofilms, Romeo T, Ed. Springer Berlin Heidelberg: Berlin, Heidelberg, 2008; pp 249–289.

53. Sugimoto S; Okuda K.-i.; Miyakawa R; Sato M; Arita-Morioka K.-i.; Chiba A; Yamanaka K; Ogura T; Mizunoe Y; Sato C Imaging of Bacterial Multicellular Behaviour in Biofilms in Liquid by Atmospheric Scanning Electron Microscopy. Sci. Rep 2016, 6, 25889. [PubMed: 27180609]

54. Yadav N; Dubey A; Shukla S; Saini CP; Gupta G; Priyadarshini R; Lochab B Graphene Oxide-Coated Surface: Inhibition of Bacterial Biofilm Formation Due to Specific Surface–Interface Interactions. ACS Omega 2017, 2 (7), 3070–3082. [PubMed: 30023683]

55. Fang Q; Chen B; Lin Y; Guan Y Aromatic and Hydrophobic Surfaces of Wood-Derived Biochar Enhance Perchlorate Adsorption Via Hydrogen Bonding to Oxygen-Containing Organic Groups. Environ. Sci. Technol 2014, 48 (1), 279–288. [PubMed: 24289306]

56. Mukherjee A; Zimmerman AR; Harris W Surface Chemistry Variations among a Series of Laboratory-Produced Biochars. Geoderma 2011, 163 (3), 247–255.

57. Rivera-Utrilla J; Bautista-Toledo I; Ferro-García MA; Moreno-Castilla C Activated Carbon Surface Modifications by Adsorption of Bacteria and Their Effect on Aqueous Lead Adsorption. Journal of Chemical Technology & Biotechnology 2001, 76 (12), 1209–1215.

58. van Loosdrecht MC; Lyklema J; Norde W; Zehnder AJ Influence of Interfaces on Microbial Activity. Microbiol. Rev 1990, 54 (1), 75–87. [PubMed: 2181260]

59. Rouquerol J; Llewellyn P; Rouquerol F, Is the BET Equation Applicable to Microporous Adsorbents? In Stud. Surf. Sci. Catal, Llewellyn PL; Rodriquez-Reinoso F; Rouqerol J; Seaton N, Eds. Elsevier: 2007; Vol. 160, pp 49–56.

60. Vander Heiden MG; Cantley LC; Thompson CB Understanding the Warburg Effect: The Metabolic Requirements of Cell Proliferation. Science 2009, 324 (5930), 1029–1033. [PubMed: 19460998]

61. Zhang H; Du W; Peralta-Videa JR; Gardea-Torresdey JL; White JC; Keller A; Guo H; Ji R; Zhao L Metabolomics Reveals How Cucumber (Cucumis Sativus) Reprograms Metabolites to Cope with Silver Ions and Silver Nanoparticle-Induced Oxidative Stress. Environ. Sci. Technol 2018, 52 (14), 8016–8026. [PubMed: 29898596]

62. Warnock DD; Lehmann J; Kuyper TW; Rillig MC Mycorrhizal Responses to Biochar in Soil – Concepts and Mechanisms. Plant Soil 2007, 300 (1), 9–20.
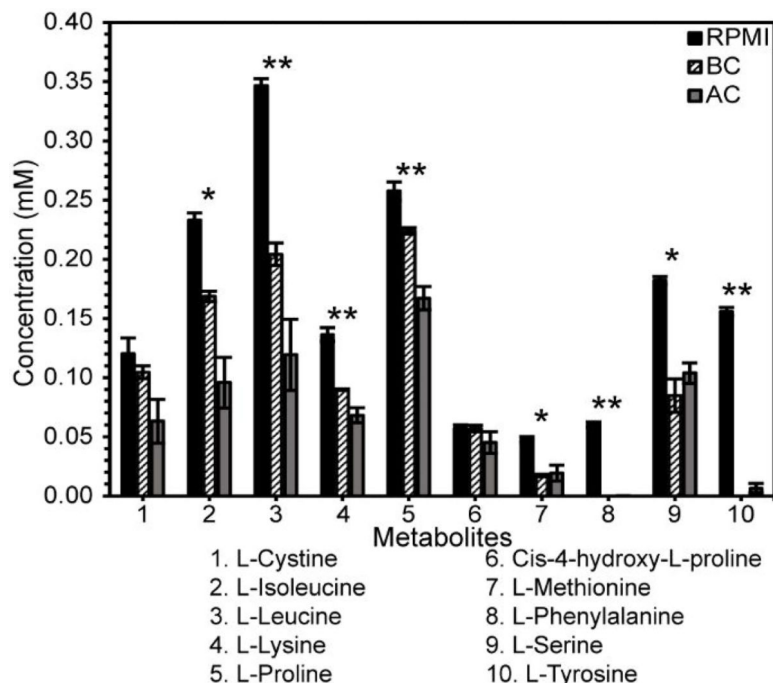
Figure 1. Initial Metabolite Concentration in Media Immediately after Treatment with Biochar or Activated Carbon.

The initial concentrations of (1) L-Cystine, (2) L-Isoleucine, (3) L-Leucine, (4) L-Lysine, (5) L-Proline, (6) Cis-4-hydroxy-L-proline, (7) L-Methionine, (8) L-Phenylalanine, (9) L-Serine, and (10) L-Tyrosine in RPMI (control, solid black), BC (diagonally striped, black and white), and AC (dark gray) media 5 min after initial mixing. Error bars are the standard error of the mean of three independently prepared samples. One-way ANOVA with Tukey's HSD test was used to identify the significant differences between RPMI and either BC- or AC-treated media. A single asterisk (*) indicates that the RPMI concentration is significantly different from both AC and BC media at a p-value < 0.05. A double asterisk (**) indicates a p-value < 0.005. The differences shown between concentrations in AC- and BC-treated media were not statistically significant for initial adsorption.
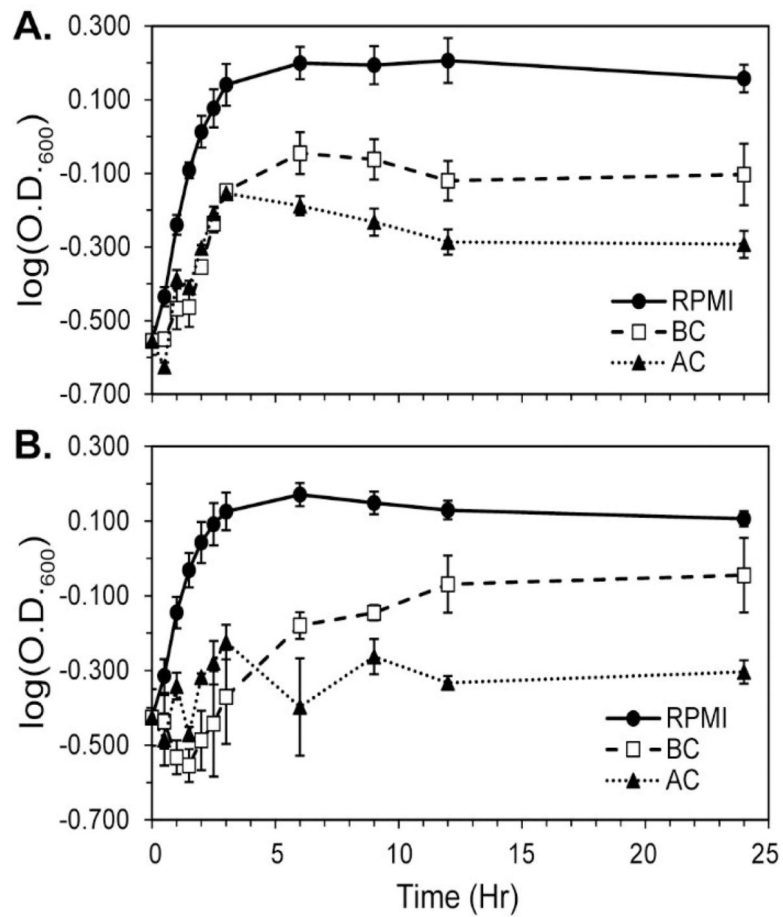
Figure 2. Growth curves of *E. coli* in RPMI Media.
Growth curves of *E. coli* in (A) unfiltered and (B) filtered RPMI media (black dots with solid black line), BC-treated RPMI media (open black squares with a dashed black line), and AC-treated RPMI media (black triangles with a dotted black line). In the filtered experiments, BC and AC are removed before growth occurs. Error bars are the standard error of the mean of three identically prepared samples.
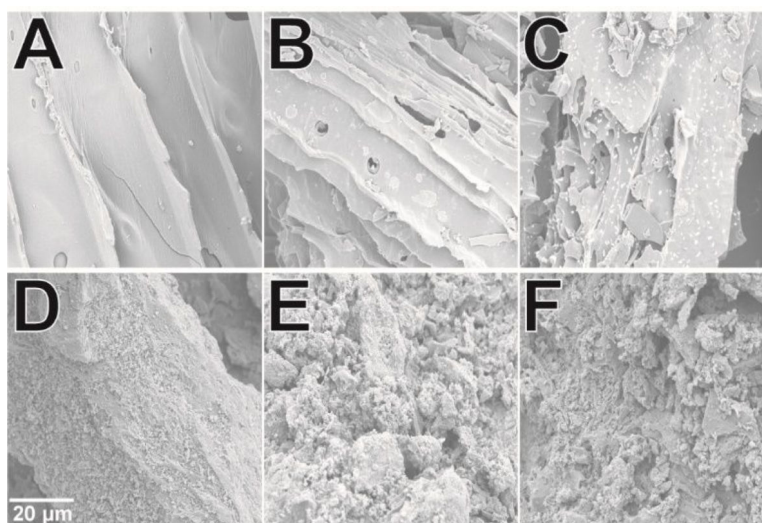
Figure 3. SEM of Bacterial Interactions with Biochar and Activated Carbon.
(A) Douglas fir, Ultra-Rinsed Black Owl Biochar (BC), (B) BC in RPMI media, (C) BC in RPMI media with *E. coli*, (D) Norit Activated Carbon (AC), (E) AC in RPMI media, and (F) AC in RPMI media with *E. coli*. The surface morphologies were studied at 5 kV. The 20 μm scale in (D) was used for all the other figures as well.
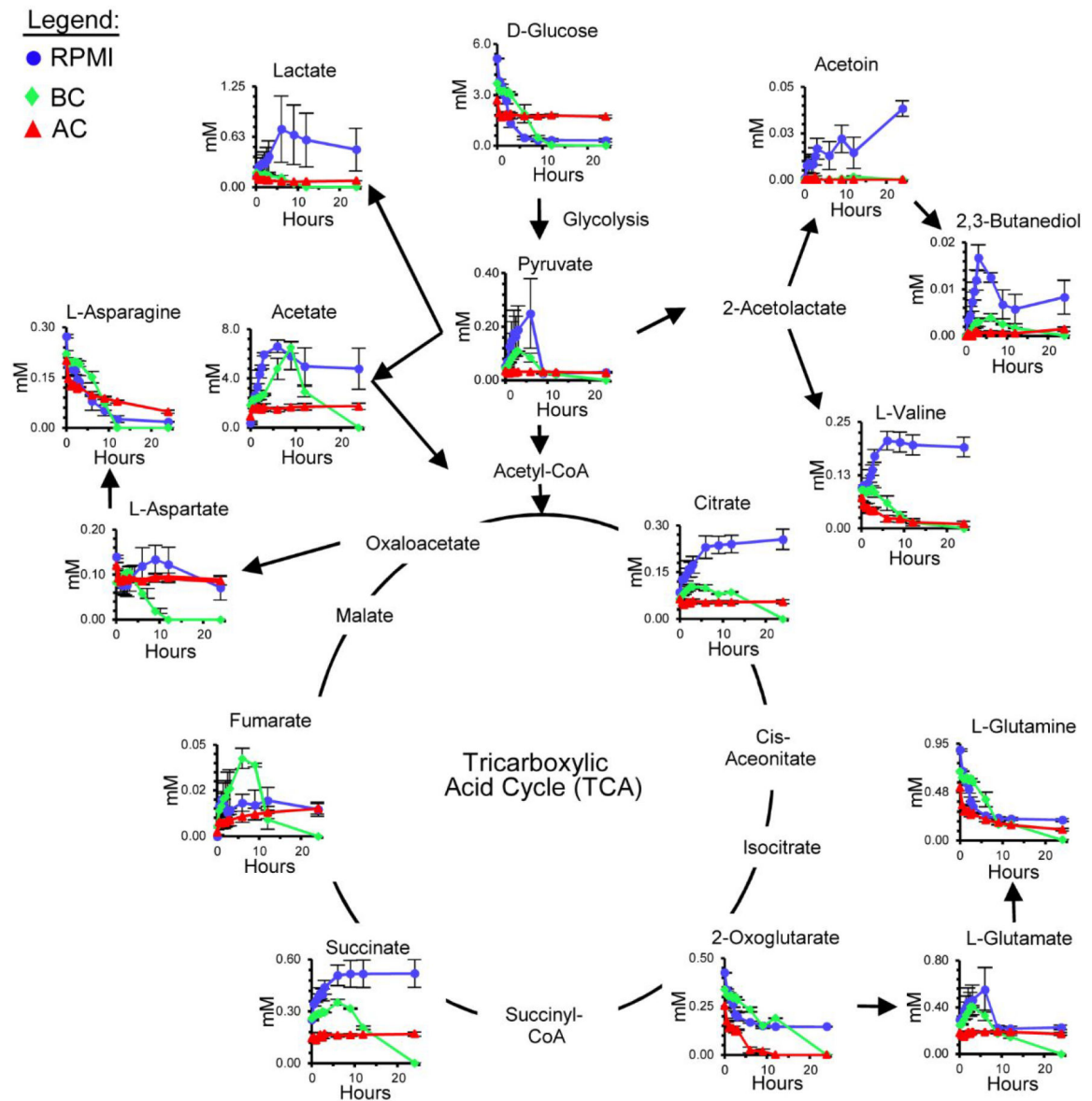
Figure 4. Tricarboxylic Acid (TCA) Cycle of *E. coli*.
The extracellular metabolite concentrations of *E. coli* in RPMI (blue), BC (green), and AC (red) media, arranged with respect to common metabolic pathways. Error bars are the standard error of the mean for three identically prepared samples.
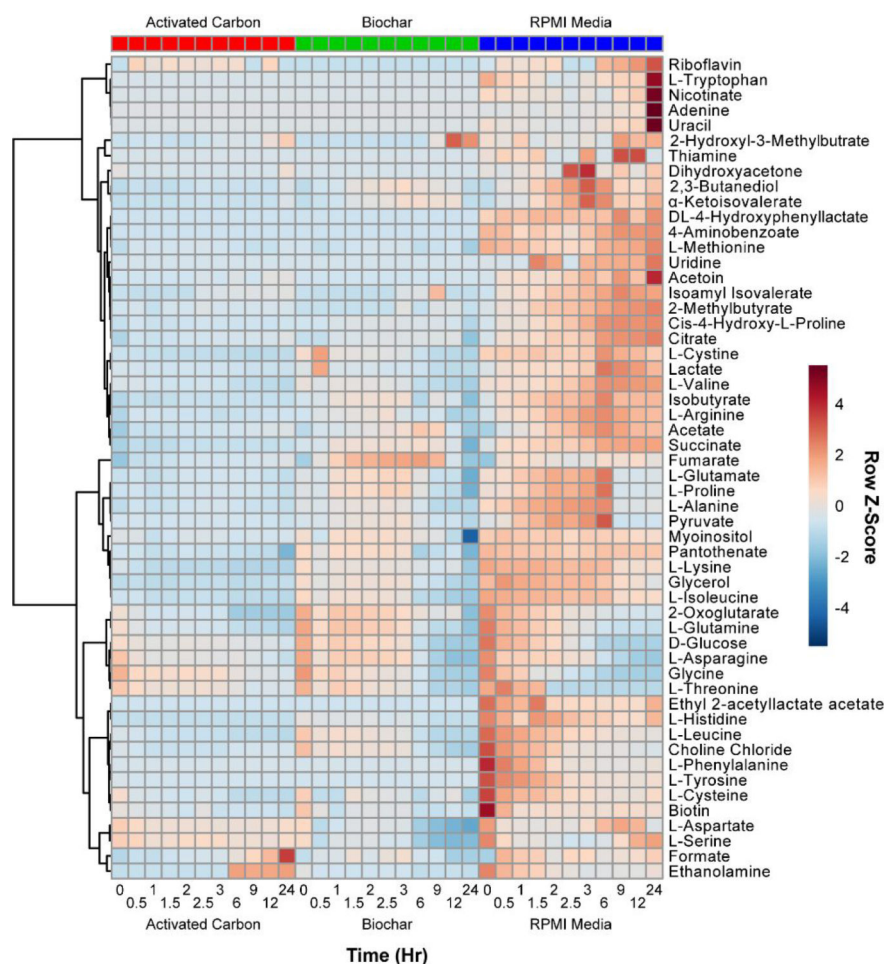
Figure 5. Heatmap of Extracellular Metabolites in Unfiltered Media.
Heatmap of extracellular metabolites' relative concentrations versus time. The row Z-score for each feature was used to color code the map: absent to low concentration metabolites were colored blue and high concentration metabolites were colored red. Ward's linkage algorithm ranked the metabolites in a clustering tree. The red boxes were labeled as AC-treated media as time increases from 0 to 24 h going left to right. The green boxes were BC-treated media and the blue boxes were RPMI media. Data are the mean values of metabolite concentrations of three replicates after being normalized using Pareto scaling.
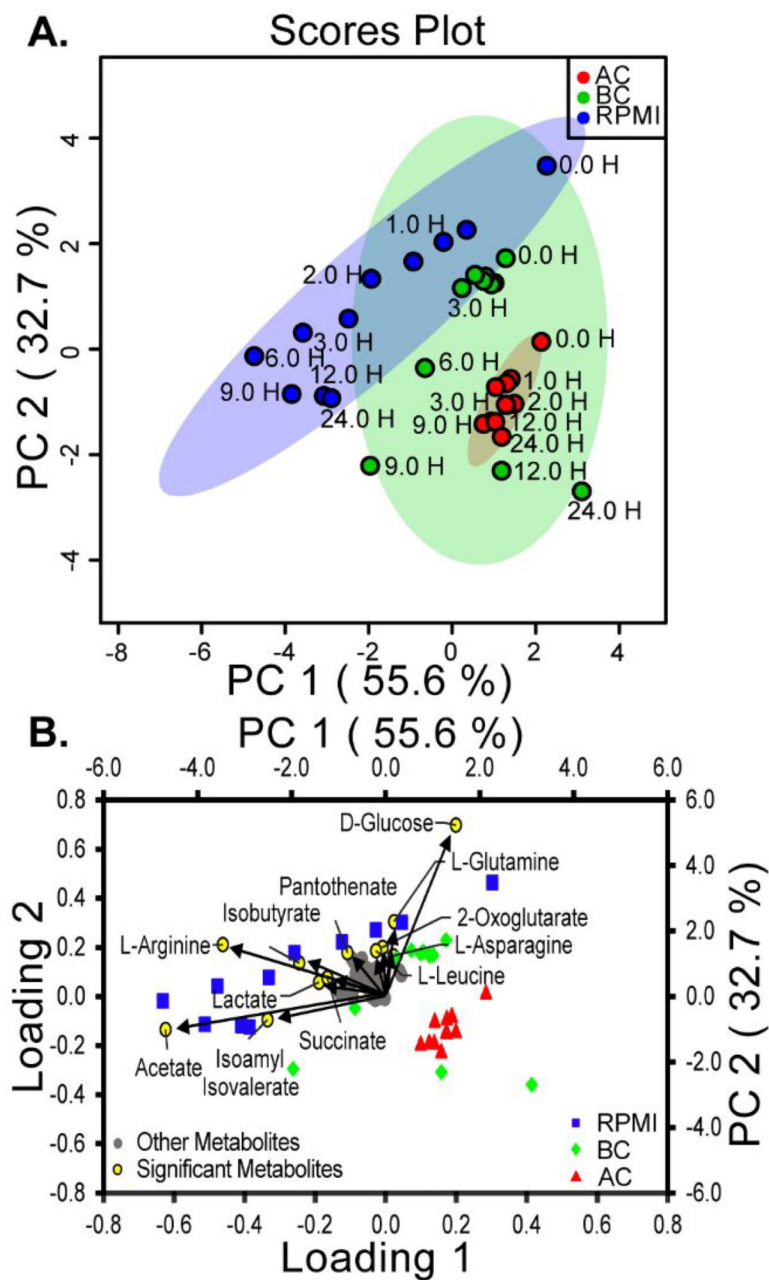
Figure 6. Statistical Analysis of *E. coli* in Unfiltered RPMI Media.
(A) A principal component analysis (PCA) scores plot on *E. coli* growth in unfiltered media was used to identify statistical differences between each media type. The shaded oval represents the 95% confidence limit for each media type (RPMI, blue circles; BC-treated media, green circles; AC-treated media, red circles). Time points for each hour are labeled, but points at half hour intervals are not labeled for clarity. (B) The metabolites in the loading plot (left and lower axes) overlaid on the PCA biplot (right and upper axes) for unfiltered media. Yellow dots represent the significant metabolites ($p < 0.05$), i.e. those making the

largest contribution to each principal component (RPMI, blue squares; BC-treated media, green diamonds; AC-treated media, red triangles).

Table 1.

BET Particle Size Analysis.

	Surface Area (SA) (m²/g)	Total Pore Volume (cm³/g)	Mean Pore Size (Å)
Black Owl Biochar	510 ± 9	0.21 ± 0.01	15.0 ± 0.1
Activated Carbon	704 ± 16	0.42 ± 0.07	16.1 ± 0.6

Standard error of the mean of three independently prepared samples.